

Extended common-image-point gathers for anisotropic imaging with blended sources

Jeff Godwin and Paul Sava (Colorado School of Mines)

Introduction

In regions characterized by complex geology, the accuracy of imaging is controlled by the quality of the Earth model used to simulate wave propagation in the subsurface (Gray et al., 2001). Thus, accurate model building is a critical prerequisite for imaging of the interior of the Earth. This requirement is even more stringent in regions characterized by strong anisotropy. Furthermore, it is important to construct subsurface velocity models using techniques that are consistent with the methods used for imaging. As reported in the recent literature, in the context of wavefield-based imaging, there are two main strategies that can be used for velocity estimation from surface seismic data. Those methods can be separated into two groups: data space methods, which operate by matching the recorded data with simulated data, and image space methods, which operate by correcting image features that indicate model inaccuracies (Sava et al., 2010).

A key component for velocity estimation implemented in the image space is the analysis of image attributes which indicate inaccurate imaging. We can update the model parameters by maximizing semblance (Symes, 2009) measured in conventional common image gathers (CIGs) or in common-image-point-gathers (CIPs). The main advantage of using extended CIPs for semblance analysis is that they can be constructed at sparse locations in the image and at locations that are consistent with the complexity of the geologic structure (Sava and Vasconcelos, 2009). Furthermore, the analysis of image attributes can be done in both isotropic and anisotropic media. Here, we do not discuss the semblance properties of extended CIPs, but simply refer to their ability to indicate the accuracy of the model (Sava and Alkhalifah, 2010).

Modern seismic surveys are characterized by huge data volumes corresponding to a large number of independent field experiments (i.e. shots). The cost of wave-equation imaging is directly proportional with the number of seismic experiments, which often reaches tens of thousands. One possible strategy for cost reduction is to image combination of experiments, a technique which is often referred to as imaging with blended sources. Blending can occur in the field or can be simulated during the imaging step (Hampson et al., 2008; Berkhout et al., 2008). Imaging with blended sources reduces the computational cost by a factor proportional with the number of experiments imaged simultaneously (Romero et al., 2000). However, this cost reduction is at the expense of the presence of cross-talk artifacts in the migrated image. These artifacts are usually attenuated simply by stacking a large number of combined experiments (Liu, 1999; Perrone and Sava, 2009).

In the context of migration velocity analysis, a natural question to ask is whether the blended sources lead to CIGs or CIPs that can be used for velocity model building. This is the topic of this abstract. We frame this discussion in the context of anisotropic model building, although a similar discussion could be carried-out for isotropic models.

Extended imaging

Wave-equation imaging can be formulated as a process involving two steps: wavefield reconstruction and the application of an imaging condition. The key elements in this imaging procedure are the source and receiver wavefields, W_s and W_r . We can represent those wavefields as 4-dimensional objects, either in the time domain as a function of space $\mathbf{x} = \{x, y, z\}$ and time t , or in the frequency domain as a function of space and frequency ω . This framework holds regardless of whether the wavefields are reconstructed

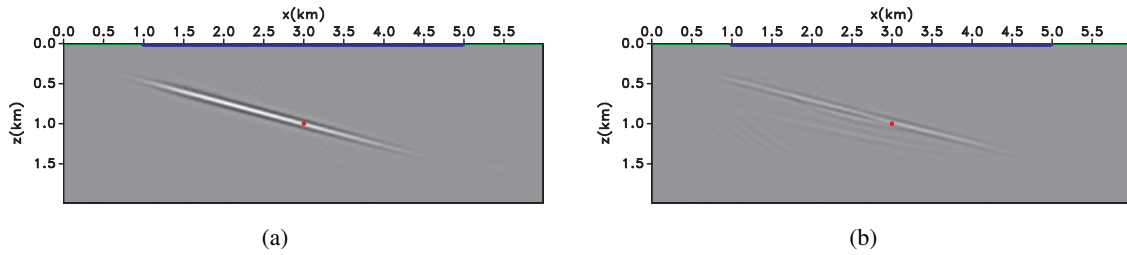
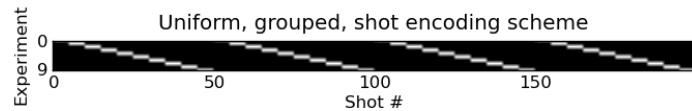


Figure 1: Images obtained by blended-source migration using 4 groups, with 5 shots per group for (a) isotropic modeling and migration, and (b) TTI modeling and isotropic migration.

Figure 2: Example of a zero time-delay encoding scheme. For each experiment, we select 20 shots in 4 groups (5 per group) that are next to each other. The groups are evenly separated in space.



using an isotropic or an anisotropic wave-equation. In this paper, we concentrate on the case of imaging using a pseudo-acoustic wave-equation (Alkhalifah, 2000; Fowler et al., 2010).

An image can be extracted from the reconstructed wavefields by the application of an extended imaging condition (Sava and Vasconcelos, 2009):

$$R(\mathbf{x}, \boldsymbol{\lambda}, \tau) = \sum_{shots} \sum_{\omega} \overline{W_s(\mathbf{x} - \boldsymbol{\lambda}, \omega)} W_r(\mathbf{x} + \boldsymbol{\lambda}, \omega) e^{2i\omega\tau}. \quad (1)$$

The image R is a function of the space coordinates \mathbf{x} , and of the space- and time-lag extensions, $\boldsymbol{\lambda}$ and τ (Rickett and Sava, 2002; Sava and Fomel, 2006). Extended images can also be used for angle decomposition (Sava and Fomel, 2003). For correct velocity, the space- and time-lag gathers are focused at the origin, and the angle-gathers are flat indicating image invariance with angle of incidence. This idea is usually referred to as the semblance principle.

The properties of the extended images constructed in anisotropic and isotropic media are different from one another. However, if we constrain the tilt of the TTI symmetry axis to be normal to the dip, then the incidence and reflection angles on the source and receiver sides are equal (Alkhalifah and Sava, 2010). Therefore, assuming that imaging is performed using an accurate subsurface model, we do not need to distinguish between isotropic and anisotropic extended images.

Cross-talk

When imaging blended sources, the cross-correlation imaging condition allows the interference of wavefields corresponding to different shots. This interference manifests itself as cross-talk, i.e. non-physical reflectors usually oriented at steep dips relative to the geologic structure. This cross-talk is inconsistent from one experiment to another, therefore it can be attenuated by stacking. However, a similar cross-talk attenuation does not occur in extended images. This remains true regardless of whether extended images are constructed at fixed surface positions, i.e. in common-image-gathers, or at fixed subsurface positions, i.e. in common-image-point-gathers.

Figures 1(a)-5(b) illustrate the cross-talk problem. The synthetic experiment uses 10 wave-equation migrations of 20 blended sources each, i.e. a total of 200 shots, encoded using the scheme shown in Figure 2. We consider two situations: first, we model and migrate with an isotropic model (constant velocity) to simulate correct imaging, Figure 1(a); second, we model using a TTI model with $\eta = 0.3$ and tilt angle $\theta = 15^\circ$, but migrate using an isotropic model to simulate incorrect anisotropic imaging, Figure 1(b). As discussed earlier, the cross-talk is not visible in the images due to its cancellation through stacking.

In contrast, Figures 4(a)-4(b) show lag-domain CIGs constructed for the isotropic modeling and migration and for TTI modeling and isotropic migration, respectively. As expected, imaging with a

Figure 3: Lag-domain CIGs located at $x = 3.0$ km in Figures 1(a) and 1(b), respectively. Cross-talk is present in the lag-gathers due to the interference between the reconstructed wavefields for separate experiments.

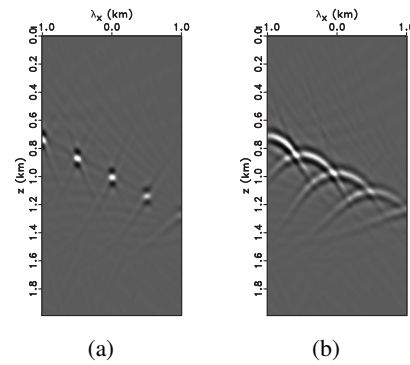
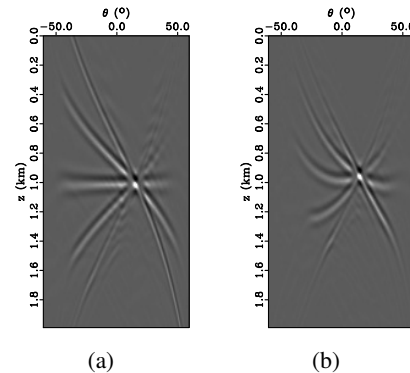


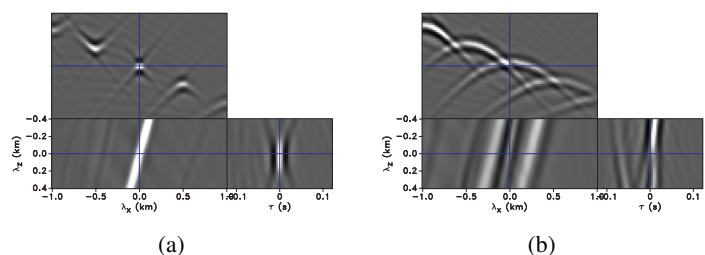
Figure 4: Angle-domain CIGs at the same locations as the CIGs shown Figures 4(a) and 4(b), respectively. Cross-talk is present in the angle-gathers due to the interference between the reconstructed wavefields for separate experiments.



correct model leads to focused events at zero lag, but imaging with an incorrect model leads to defocused events. However, the even more interesting feature of these CIGs is that we see several replications of the focused event at zero lag. These events are separated by a distance along the lag axis proportional to the shot separation in the blended experiments. Furthermore, the replications are distributed in space consistent with the underlying reflector, and the artifacts observed in the lag-domain CIGs also appear as artifacts in the angle domain, Figures 5(a)-5(b). This is not a surprise since the angle gathers are simply obtained by remapping the lag-domain CIGs (Sava and Fomel, 2003). Finally, a similar behavior is visible in extended CIPs constructed at fixed locations in the subsurface, as shown in Figures 6(a) and 6(b), respectively.

The replications observed in CIGs or CIPs can be explained by the procedure used for constructing the extended images. Equation 1 suggests that the extended images are constructed by cross-correlation of reconstructed wavefields in the subsurface. In blended-source imaging, the reconstructed wavefields simultaneously contain information due to different seismic experiments. By shifting the wavefields in space using the lag distance λ , the wavefields from different experiments are allowed to interfere with one-another and produce cross-talk. An intuitive hint of this process is given by the fact that the lag-domain replications are separated by a distance equal to half of the separation between the shots simultaneously imaged, Figure 2. A similar, but more complex phenomenon, characterizes the CIPs for which the wavefields are translated relative to one-another not only in space, but also in time.

Figure 5: Extended CIPs obtained by blended-source migration using 4 groups, with 5 shots per group for (a) isotropic modeling and migration, and (b) TTI modeling and isotropic migration. The extended CIP gathers are constructed at the (red) dot shown in Figures 1(a) and 1(b), respectively.



Finally, we can ask the question: why does this matter? The reason is that conventional velocity model building procedures do not account for the presence of multiple interfering events in CIGs or CIPs. For example, a conventional MVA procedure based on the semblance principle penalizes all image energy found away from zero-lag (Symes, 2009). For blended-source imaging, this procedure is not applicable since strong replications of the main event exist at non-zero space- and time-lags even when imaging is performed using a correct model.

Conclusions

The cross-talk artifacts due to conventional imaging with blended sources are attenuated by stacking over multiple groups of experiments. However, extended CIGs and CIPs contain additional events which are replications of the main reflections due to the sparse grouping of the blended sources. Such events are due to cross-talk of seismic energy corresponding to different experiments and hamper conventional migration velocity analysis. The separation between the multiple events present in extended images is proportional to the separation between the blended sources. Therefore, for model building applications, we could design an optimal separation of the shots in blended experiments thus avoiding cross-talk in extended images.

Acknowledgments

This work is supported by the sponsors of the Center for Wave Phenomena at Colorado School of Mines.

REFERENCES

- Alkhalifah, T., 2000, An acoustic wave equation for anisotropic media: *Geophysics*, **65**, 1239–1250.
- Alkhalifah, T., and P. Sava, 2010, A transversely isotropic medium with a tilted symmetry axis normal to the reflector: *Geophysics (Letters)*, in press.
- Berkhout, A. J. G., G. Blacquiére, and E. Verschuur, 2008, From simultaneous shooting to blended acquisition: *SEG Technical Program Expanded Abstracts*, **27**, 2831.
- Fowler, P. J., X. Du, and R. P. Fletcher, 2010, Coupled equations for reverse time migration in transversely isotropic media: *Geophysics*, **75**, S11–S22.
- Gray, S. H., J. Etgen, J. Dellinger, and D. Whitmore, 2001, Seismic migration problems and solutions: *Geophysics*, **66**, 1622–1640.
- Hampson, G., J. Stefani, and F. Herkenhoff, 2008, Acquisition using simultaneous sources: *The Leading Edge*, **27**, 918.
- Liu, F., 1999, Plane wave source composition: An accurate phase encoding scheme for prestack migration: *SEG Technical Program Expanded Abstracts*, **21**, 1156.
- Perrone, F., and P. Sava, 2009, Comparison of shot encoding functions for reverse-time migration: *SEG Technical Program Expanded Abstracts*, 2980–2984.
- Rickett, J., and P. Sava, 2002, Offset and angle-domain common image-point gathers for shot-profile migration: *Geophysics*, **67**, 883–889.
- Romero, L. A., D. C. Ghiglia, C. C. Ober, and S. A. Morton, 2000, Phase encoding of shot records in prestack migration: *Geophysics*, **65**, 426.
- Sava, P., and T. Alkhalifah, 2010, Extended common-image-point gathers for anisotropic wave-equation migration: Presented at the 72nd Annual Meeting, EAGE, Pre-convention workshop "Migration Velocity Analysis in Anisotropic Media What Is Possible and What Is Impossible".
- Sava, P., and S. Fomel, 2003, Angle-domain common image gathers by wavefield continuation methods: *Geophysics*, **68**, 1065–1074.
- , 2006, Time-shift imaging condition in seismic migration: *Geophysics*, **71**, S209–S217.
- Sava, P., P. Fowler, and U. Albertin, 2010, Objective functions for seismic wavefield tomography: *Geophysics (Letters)*, submitted for publication.
- Sava, P., and I. Vasconcelos, 2009, Extended imaging condition for wave-equation migration: *Geophysical Prospecting*, submitted for publication.
- Symes, W., 2009, Migration velocity analysis and waveform inversion: *Geophysical Prospecting*, **56**, 765–790.